

# Multidrug-resistant Human Sarcoma Cells with a Mutant P-Glycoprotein, Altered Phenotype, and Resistance to Cyclosporins\*

(Received for publication, August 22, 1996, and in revised form, December 10, 1996)

Gang Chen, George E. Durán, Katherine A. Steger, Norman J. Lacayo, Jean-Pierre Jaffrézou, Charles Dumontet, and Branimir I. Sikic‡

From the Divisions of Oncology and Clinical Pharmacology, Department of Medicine, Stanford University School of Medicine, Stanford, California 94305-5306

**A variant of the multidrug-resistant human sarcoma cell line Dx5 was derived by co-selection with doxorubicin and the cyclosporin D analogue PSC 833, a potent inhibitor of the multidrug transporter P-glycoprotein. The variant DxP cells manifest an altered phenotype compared with Dx5, with decreased cross-resistance to Vinca alkaloids and no resistance to dactinomycin. Resistance to doxorubicin and paclitaxel is retained. The multidrug resistance phenotype of DxP cells is not modulated by 2  $\mu$ M PSC 833 or cyclosporine. DxP cells manifest a decreased ability to transport [ $^3$ H]cyclosporine. DNA heteroduplex analysis and sequencing reveal a mutant *mdr1* gene (deletion of a phenylalanine at amino acid residue 335) in the DxP cell line. The mutant P-glycoprotein has a decreased affinity for PSC 833 and vinblastine and a decreased ability to transport rhodamine 123. Transfection of the mutant *mdr1* gene into drug-sensitive MES-SA sarcoma cells confers resistance to both doxorubicin and PSC 833. Our study demonstrates that survival of cells exposed to doxorubicin and PSC 833 in a multistep selection occurred as a result of a P-glycoprotein mutation in transmembrane region 6. These data suggest that Phe<sup>335</sup> is an important binding site on P-glycoprotein for substrates such as dactinomycin and vinblastine and for inhibitors such as cyclosporine and PSC 833.**

The development of drug resistance in tumor cells is a major obstacle to clinical response in cancer chemotherapy. A well characterized cellular phenotype termed multidrug resistance (MDR)<sup>1</sup> is mediated by the multidrug transporter P-glycoprotein (P-gp), which functions as an ATP-dependent drug efflux pump of broad substrate specificity (1–3). The *mdr1* gene, which encodes P-gp, is expressed in some normal and malig-

nant tissues and has been associated with a poor prognosis in several types of cancer (4–9). The reversal of MDR by inhibitors or modulators of P-gp may improve the outcome of cancer chemotherapy (4, 9–15). Cyclosporine, its analogue PSC 833 (PSC; Refs. 13 and 14), verapamil, and other MDR modulators have been shown to increase cellular drug accumulation and reverse MDR through competitive binding to P-gp (reviewed in Refs. 2, 4, and 9). Current clinical trials using antitumor agents combined with MDR modulators to circumvent MDR have raised the issue of whether the suppression of P-gp function might result in the selection of alternative mechanisms that could confer resistance to multiple agents. These mechanisms include changes in topoisomerase (Topo) II $\alpha$  or II $\beta$  (reviewed in Refs. 16–17 and 18) and increased expression of the gene for the multidrug resistance-associated protein, *mrp* (19, 20), or the p110 major vault protein, LRP-56 (21).

In this study, we utilized co-selection to investigate the mechanisms conferring resistance to both doxorubicin (DOX) and PSC. The parental cells expressed high levels of P-gp. We hypothesized that the suppression of P-gp function might favor the emergence of an altered form of P-gp or an alternative mechanism of resistance (22, 23). Our data reveal the expression of a novel mutant P-gp in variant cells with an altered spectrum of cross-resistance to cytotoxins and resistance to modulation by cyclosporins. The resistant cells and mutant P-gp were characterized in terms of their patterns of drug resistance, modulation by inhibitors of P-gp, and transport of drugs and their P-gp expression, gene sequence, and transfection of the mutant *mdr1*.

## EXPERIMENTAL PROCEDURES

**Drugs and Chemicals**—Doxorubicin was obtained from Adria Laboratories (Columbus, OH), etoposide from Bristol-Myers (Evansville, IN), and vinblastine from Eli Lilly and Co. (Indianapolis, IN). PSC was provided by Sandoz Pharmaceutical Corporation (Basel, Switzerland). Rhodamine 123 (Rh-123) was purchased from Molecular Probes (Eugene, OR). All other anti-cancer agents were obtained from the NCI (National Institutes of Health), and all other chemicals were from Sigma.

**Cells and Tissue Culture**—Details of the development and characterization of the human cell line MES-SA and its MDR variant MES-SA/Dx5 (Dx5), which were derived from sarcoma elements of a uterine mixed Mullerian tumor, have previously been described (24, 25). MES-SA/DxP5002 (DxP) cells were derived from Dx5.05 cells (Dx5 cells selected and maintained at a DOX concentration of 0.5  $\mu$ M) by stepwise selection in the presence of increasing DOX concentrations (from 40 nM to 0.5  $\mu$ M) and a constant PSC concentration at 2  $\mu$ M over a 1-year period.

**Cytogenetic Analysis and Fluorescence in Situ Hybridization**—Metaphase chromosome preparations were examined for the presence and structure of chromosome 7, where the human *mdr1* gene is normally located, by karyotyping and *in situ* hybridization with a chromosome 7-specific probe (Oncor, Inc., Gaithersburg, MD). The hybridized chromosome was visualized by the method of Sasai *et al.* (26) using fluorescence microscopy.

\* This work was supported in part by American Cancer Society Grant DHP-76 and National Institutes of Health Grant RO-1 CA 52168. The costs of publication of this article were defrayed in part by the payment of page charges. This article must therefore be hereby marked "advertisement" in accordance with 18 U.S.C. Section 1734 solely to indicate this fact.

‡ To whom correspondence and reprint requests should be addressed: Room M-211, Oncology Division, Stanford University Medical Center, Stanford, CA 94305-5306. Tel.: 415-725-6427; Fax: 415-725-1420; E-mail: mv.bis@forsythe.stanford.edu.

<sup>1</sup> The abbreviations used are: MDR, multidrug resistance; DOX, doxorubicin; Dx5, the multidrug-resistant cell line MES-SA/Dx5; DxP, the multidrug-resistant variant cell line MES-SA/DxP; IC<sub>50</sub>, drug concentration resulting in 50% inhibition of MTT dye formation compared with controls; PCR, polymerase chain reaction; RT-PCR, reverse transcriptase-PCR; P-gp, P-glycoprotein; PSC, the cyclosporin D analogue PSC 833; TM5, -6, -11, and -12, fifth, sixth, eleventh, and twelfth transmembrane regions of P-glycoprotein, respectively; Topo, topoisomerase; Rh-123, rhodamine 123; MTT, (3-[4,5-dimethylthiazol-2-yl]-2,5-diphenyl tetrazolium bromide).

TABLE I  
Oligonucleotides used in amplification and detection of *mdr1* cDNA

Amplimers <sup>a</sup>	Location	Sequence
Humdr1-F <sup>b</sup>	181-199	5'-ATGGATCCGGCCGGGAGCAGTCATCTG-3'
Humdr1-F	421-440	5'-ATGGATCCCGGGATGGATCTGAAGGGG-3'
Humdr1-R <sup>c</sup>	476-495	5'-CTGAATCCACTTTTATTGTTTCAGTTT-3'
Humdr1-F	714-735	5'-ATGGATCCATATCAATGATACAGGGTTCTT-3'
Humdr1-R	822-841	5'-CTGAATTCCTGCCAGGCACAAAATGAAA-3'
Humdr1-F	951-971	5'-ATGGATCCAGATGATGTCTTAAGATTA-3'
Humdr1-F	1194-1213	5'-ATGGATCCTCTTGGCAGCAATTAGAACT-3'
Humdr1-R	1238-1257	5'-CTGAATTCCTGTACCTTTCAAGTTCTTT-3'
Humdr1-F	1460-1477	5'-ATGGATCCGGACAGGCATCTCCAAGC-3'
Humdr1-R	1501-1519	5'-CTGAATTCGATTTTCATAAGCTGCTCCT-3'
Humdr1-F	1702-1721	5'-ATGGATCCTGGAACAGTGGCTGTGGGA-3'
Humdr1-R	1703-1721	5'-CTGAATTCCTCCACAGCCACTGTTTCC-3'
Humdr1-R	2025-2043	5'-CTGAATTCGCGATCCTCTGCTTCTGC-3'
Humdr1-R	2226-2247	5'-CTGAATTCCTCCACAATGACTCCATCATC-3'
Linker-F	2228-2247	5'-CGATGATGGAGTCATTGTGGA-3'
Humdr1-R	2433-2450	5'-CTGAATTCGTGATCCACGGACACTCC-3'
Linker-R	2593-2614	5'-TATTGCAAATGCTGGTTGCAGG-3'
Humdr1-F	2593-2614	5'-ATGGATCCCTGCAACCAGCATTTGCAATA-3'
Humdr1-F	2797-2814	5'-ATGGATCCGGTTTTCCGATCCATGCT-3'
CP482-F	3020-3039	5'-CCCATCATTGCAATAGCAGG-3'
CP483-R	3168-3187	5'-AGCATACATATGTTCAAACCT-3'
Humdr1-F	3105-3124	5'-ATGGATCCGGAAGATCGCTACTGAAGCA-3'
Humdr1-F	3395-3415	5'-ATGGATCCGTGATTCATTGCTCCTGAC-3'
Humdr1-R	3402-3421	5'-CTGAATTCGGCATAGTCAGGAGCAAATG-3'
Humdr1-F	3705-3724	5'-ATGGATCCTGCTGCTTGTGGCAAAGAA-3'
Humdr1-R	3768-3788	5'-CTGAATTCGGATGGGCTCCTGGGACACGA-3'
Humdr1-R	4043-4062	5'-CTGAATTCACCTTTTCACTTCTGTATC-3'
Humdr1-R	4250-4269	5'-CTGAATTCGTTCACTGGCGCTTTGTTC-3'
Humdr1-R	4380-4398	5'-ATGGATCCCTCTGAACCTTGACTGAGG-3'
Humdr1-R	4548-4570	5'-CTCTCGAGCAAGGCAGTCAGTTACAGTCCA-3'

<sup>a</sup> Amplimers were designed according to a previously published sequence (26). The boldface bases in amplimers represent the restriction sites of *Bam*HI, *Eco*RI, or *Xho*I for facilitating subcloning.

<sup>b</sup> F, forward amplimers.

<sup>c</sup> R, reverse amplimers.

TABLE II  
The multidrug resistance phenotype of Dx5 and DxP cells

Cytotoxin	-Fold Resistance <sup>a</sup>			
	MES-SA	Dx5	DxP	Dx5/DxP <sup>b</sup>
Anthracyclines				
Daunorubicin	1 (20) <sup>c</sup>	75	25	3
Doxorubicin	1 (40)	80	77	1
Anti-microtubule				
Colchicine	1 (1)	79	75	1
Paclitaxel	1 (1)	175	100	2
Vinblastine	1 (4)	243	14	17
Vincristine	1 (2)	199	8	25
Vinorelbine	1 (60)	17	2	9
Epipodophyllotoxins				
Etoposide	1 (500)	42	17	2
Teniposide	1 (100)	135	53	3
Others				
Amsacrine	1 (100)	26	2	13
Dactinomycin	1 (0.3)	183	1	183

<sup>a</sup> -Fold resistance was determined as described under "Experimental Procedures." Values are the means of at least three to six independent experiments.

<sup>b</sup> -Fold resistance difference in DxP cells compared with parental Dx5 cells.

<sup>c</sup> Values in parenthesis represent the IC<sub>50</sub> values (nM of drug-sensitive MES-SA cells).

**Growth Inhibition Assay and Reversal of MDR by Modulators**—Growth inhibition and doubling times were evaluated by the MTT colorimetric assay in triplicate or quadruplicate as described previously (22, 23). The modulation of resistance to DOX, paclitaxel, vinblastine, and etoposide was also determined by MTT assays in the presence of the MDR modulator PSC (2 μM) or verapamil 6 μM. These concentrations of the modulators are noncytotoxic and completely reverse resistance to DOX in our cellular MDR models. The modulation ratio was obtained by comparing IC<sub>50</sub> values in the presence and absence of modulators (22).

**Cellular Accumulation of [<sup>3</sup>H]Daunorubicin, [<sup>3</sup>H]Vinblastine, and [<sup>3</sup>H]Cyclosporine**—Intracellular drug accumulation was quantified using radiolabeled drugs as described previously (23). All values were normalized to protein content.

**Flow Cytometric Analysis**—The flow cytometric analysis of Rh-123

retention and P-gp expression were determined by a dual laser flow cytometer (FACS-II<sup>TM</sup>; Becton-Dickinson Corp., Mountain View, CA). Double labeling was performed with Rh-123 and the monoclonal antibody UIC2 Immunotech, Inc. (Westbrook, ME).

**Amplimers Used for Reverse Transcriptase-Polymerase Chain Reaction (RT-PCR)**—The oligonucleotides used as amplimers in this study were synthesized by Operon Technologies (Alameda, CA) and Ana-Gen Inc. (Palo Alto, CA). The sets of amplimers specific for Topo IIα and IIβ protein and *mnp* have been previously documented (22, 23). A panel of *mdr1* primers for mRNA sequence amplification was designed according to the published sequence (27) and is summarized in Table I. 28 S ribosomal cDNA was used as an endogenous control for PCR (22, 23).

**RT-PCR**—The isolation of total RNA and procedures of RT-PCR were performed as previously reported (22, 23). PCR conditions for each pair of primers were determined by evaluating the linearity of the genera-

tion of PCR products with serial dilutions of cDNA (5, 25, 50, and 100 ng per reaction). Reactions were determined to be in the linear range of amplification by comparison of at least two dilutions of each sample and two cycle end points. All PCR experiments were performed on RNAs from several different preparations.

**DNA Heteroduplex Analysis and PCR Sequencing**—*mdr1* PCR products were subjected to heteroduplex analysis using the mutation detection enhancement system (J.T. Baker Inc.). An 8–12% MDE™ Gel (J.T. Baker) was used and stained with ethidium bromide, and the desired products were located on an ultraviolet transilluminator and photographed. The results were further assessed by DNA sequencing of the PCR products (Amersham Life Science Inc.). Sequences were obtained from several preparations of cDNA, and these were compared with the parental cell line, Dx5 and the published human *mdr1* sequence (27).

**Genomic DNA PCR, Heteroduplex, Subcloning, and Sequencing**—In order to identify the presence of the mutation in genomic DNA of DxP cells, we isolated genomic DNA from MES-SA, Dx5, and DxP cells. The PCR products were obtained by amplifying the target region using genomic specific primers located in introns 9 and 10, which are adjacent to exon 10 of *mdr1*: forward primer, 5'-ATGGATCCTCTTCACATTCC-TCAGGTAT-3'; reverse primer, 5'-CTCTCGAGGGCCAACTCAGACT-TACATTAT-3' (27). Heteroduplex analysis was performed, and heteroduplex bands were subjected to PCR reamplification. The bands were purified from 8% polyacrylamide gel and subcloned into the pGEM-T vector (Promega). Individual clones were selected for sequencing.

**Western Blotting of P-gp and Topo II $\alpha$** —Western blotting with chemiluminescent detection (ECL kit, Amersham Corp.) was used for the analysis of P-gp and Topo II $\alpha$  proteins. Total cell lysates from the exponentially growing cells were used for P-gp immunoblotting (22, 23), and a nuclear protein extract, prepared by the methods previously described (23), was utilized in the Topo II assay.

**Immunohistochemical Analysis of P-gp and P110 Expression**—Immunohistochemical analyses were performed using the monoclonal antibodies MRK16 and C219 for P-gp and the antibody LRP-56 for the p110 major vault protein (Caltag, S. San Francisco, CA) (20, 22, 23).

**Photoaffinity Labeling with [<sup>125</sup>I]Iodoarylazidoprazosin and [<sup>3</sup>H]Azidopine**—Plasma membranes for photoaffinity labeling were prepared as described (28), followed by assays of displacement of the P-gp probes [<sup>125</sup>I]iodoarylazidoprazosin and [<sup>3</sup>H]azidopine (29). MES-SA, Dx5, and DxP cells (100  $\mu$ g of protein) were incubated with [<sup>125</sup>I]iodoarylazidoprazosin (81.4 TBq/mmol; DuPont NEN) and [<sup>3</sup>H]azidopine (Amersham) in the presence or absence of modulators in a 10 mM Tris-HCl buffer (pH 7.4) at a final volume of 50  $\mu$ l. These preparations were incubated at 25 °C for 1 h in the dark, followed by a 20-min exposure to a 254-nm UV source (UVP, Inc., San Gabriel, CA). 50  $\mu$ l of loading buffer was added, and proteins were separated on an 8% SDS-polyacrylamide gel, dried, and analyzed by autoradiography.

**Clonal Analysis of DxP Cells**—Subcloning of cells was performed by limiting dilution. Both resistant and revertant clones were analyzed for the MDR phenotype, drug accumulation, and RT-PCR or heteroduplex as described above.

**Mutant *mdr1* Transfection and Cytotoxic Assay**—A cDNA library was constructed from DxP cells in  $\lambda$ gt10 phage, and mutant *mdr1* clones were identified by hybridization, digested with *NotI*, and subcloned into the expression vector *NotI* site of pcDNA3 (Invitrogen). The plasmid pcDMDR1.4, which codes for wild-type P-gp was obtained by subcloning a *BamHI-XhoI* fragment of pMDR2000XS containing *mdr1* sequence from position -140 to position 4240 into pcDNA3 multiple cloning sites. An additional mutant *mdr1* plasmid, pcDMDR3.5, was derived by replacing a 211-base pair *NsiI-SfuI* fragment of *mdr1* from pMDR2000XS with a PCR fragment from DxP cells spanning the position Phe<sup>335</sup> deletion. Transfection of drug-sensitive MES-SA cells and K562 cells was performed by electroporation (30) and Lipofectin-mediated DNA transfer (Life Technologies, Inc.). Recipient cells ( $2 \times 10^7$ ), were transfected with 10  $\mu$ g of plasmid. In a transient transfection assay, the MDR phenotype was tested after 48 h of incubation. Stably transfected cells were obtained by selection with G418 (800  $\mu$ g/ml) for 14 days.

## RESULTS

**Establishment of the Doxorubicin- and PSC-resistant Subline**—Stepwise selection of the MDR human sarcoma cell line Dx5 in the presence of increasing DOX concentrations and constant exposure to PSC (2  $\mu$ M) resulted, over a 1-year period, in the stably DOX- and PSC-resistant cell line, DxP. Karyotypic analysis revealed 47 or 48 chromosomes in both the Dx5 and DxP cells with a similar G-banding pattern of chromosome

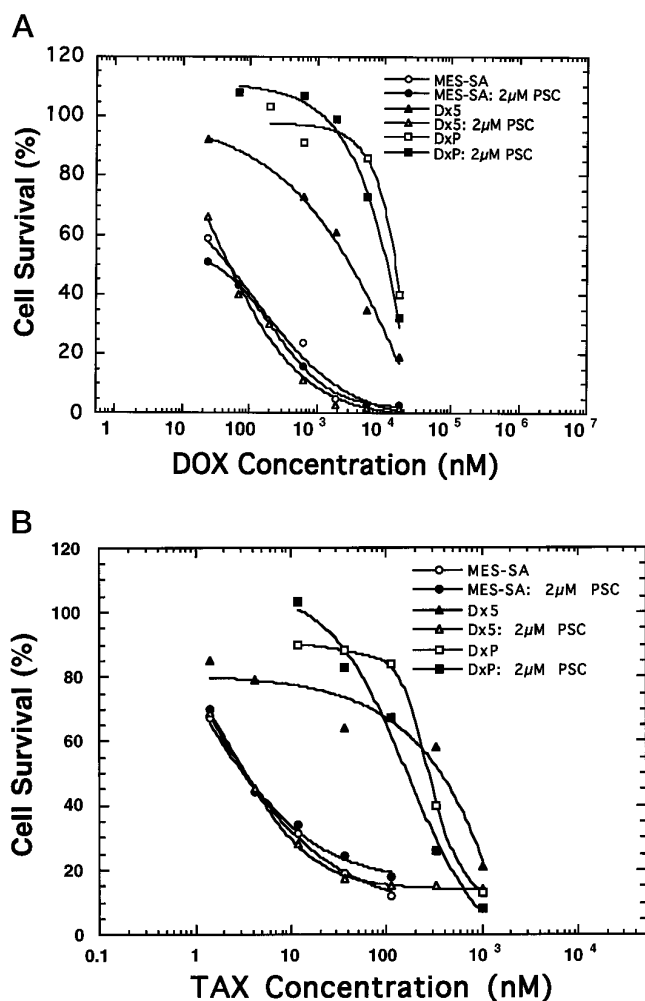


FIG. 1. Survival curves of DxP cells treated with DOX or paclitaxel with or without PSC. A, DOX with or without PSC. B, paclitaxel with or without PSC. MES-SA and Dx5 cells are used as sensitive and resistant controls, respectively. A representative experiment from at least three replicates is shown.

7 (data not shown). Fluorescence *in situ* hybridization demonstrated two copies of chromosome 7 in both Dx5 and DxP cells, whereas parental, drug-sensitive MES-SA cells have 45 chromosomes and one chromosome 7 (24, 25).

**Multidrug Resistance Phenotype**—The drug resistance phenotype of DxP cells is shown in Table II and Fig. 1. Their level of resistance to the anthracycline DOX is similar to that of the parental Dx5 cells, with a slightly decreased cross-resistance to daunorubicin. The most notable alterations were found in levels of resistance to dactinomycin and *Vinca* alkaloids. Resistance to vinblastine decreased 17-fold, to vincristine 25-fold, and to vinorelbine 9-fold (to a level similar to that of drug-sensitive MES-SA cells). Resistance to amсарine decreased 13-fold, and sensitivity to dactinomycin was completely restored. This cell line maintained high levels of resistance to colchicine and paclitaxel (Taxol®), and moderately decreased resistance to podophyllotoxins (etoposide and teniposide). There was no significant difference in cellular generation time (22 h) compared with parental Dx5 cells.

**In Vitro Modulation of MDR by PSC and Verapamil**—Modulation of resistance to several MDR-related cytotoxins by PSC (2  $\mu$ M), cyclosporine (3  $\mu$ M), and verapamil (6  $\mu$ M) was examined by the MTT assay. PSC, the most potent of the modulators used, completely restored the sensitivity of the highly multidrug-resistant cell line Dx5 to DOX, vinblastine, paclitaxel,

TABLE III  
Modulation of multidrug resistance in Dx5 and DxP cells

Cytotoxin	-Fold resistance <sup>a</sup>		
	MES-SA	Dx5	DxP
Doxorubicin	1	80	77
+2 $\mu$ M PSC	1	1	53
+3 $\mu$ M Cyclosporine	0.5	2	30
+6 $\mu$ M Verapamil	0.5	4	18
Paclitaxel	1	175	100
+2 $\mu$ M PSC	0.3–1 <sup>b</sup>	1	5
+3 $\mu$ M Cyclosporine	0.5–1	13	38
+6 $\mu$ M Verapamil	0.3–1	25	44
Vinblastine	1	243	14
+2 $\mu$ M PSC	0.3–1	1	12
+3 $\mu$ M Cyclosporine	0.5–1	6	7
+6 $\mu$ M Verapamil	0.4–1	4	3
Vincristine	1	199	8
+2 $\mu$ M PSC	0.7	1	7
+6 $\mu$ M Verapamil	0.3–1	7	3
Colchicine	1	79	75
+2 $\mu$ M PSC	1	1	70
+3 $\mu$ M Cyclosporine	1	6	30
+6 $\mu$ M Verapamil	1	12	30
Etoposide	1	42	18
+2 $\mu$ M PSC	1	1	18

<sup>a</sup> Fold resistance was determined as described under "Experimental Procedures."

<sup>b</sup> Increased sensitivity to cytotoxins was observed occasionally in MES-SA cells treated with MDR modulators, although these cells do not express *mdr1*.

vincristine, and colchicine, relative to the drug-sensitive MES-SA cells. In contrast, DxP cells were almost completely resistant to the modulating effects of PSC, substantially resistant to cyclosporine, and somewhat less resistant to modulation by verapamil (Table III, Fig. 1).

**Analysis of *mdr1*, *Topo II $\alpha$*  and *II $\beta$* , and *mrp* Expression—**Total RNA was extracted from isolated DxP clones and analyzed by RT-PCR for the presence of *mdr1*, *Topo II $\alpha$* , *Topo II $\beta$* , and *mrp* transcripts (Fig. 2). In comparison with the parental Dx5 cells, DxP displayed levels of *mdr1* transcripts similar to the parental Dx5 cells. The expression of *mrp* was compared with MES-SA and Dx5 cells and with normal human lung tissue as a positive control. A similar level of expression of *mrp* was observed in human lung tissue, MES-SA sarcoma cells (data not shown), and Dx5 and DxP cells. While no significant difference was seen in *Topo II $\alpha$*  transcripts, DxP cells manifested a 2-fold elevation of *Topo II $\beta$*  expression relative to Dx5 cells (Fig. 2).

**P-glycoprotein Expression—**P-gp expression and function were analyzed by RT-PCR, immunoblotting with the C219 antibody, and flow cytometry with the antibody UIC2 (Figs. 3 and 4). Dx5 and DxP cells displayed similarly high levels of expression of P-gp. Immunohistochemical staining of cells with the MRK16 and C219 antibodies confirmed that the expression of P-gp on DxP cells was predominantly localized to the plasma membrane and similar in amount to that observed in Dx5 cells (data not shown).

***Topo II $\alpha$*  and *p110* Expression—**Expression of *Topo II $\alpha$*  isoforms by immunoblotting revealed a slight increase in DxP compared with Dx5 cells. Neither Dx5 nor DxP cells had detectable expression of the p110 major vault protein, although the drug-sensitive MES-SA cells from which Dx5 cells were originally derived are weakly positive for p110 (data not shown).

**Rh-123 Retention and Modulation with PSC—**The cellular accumulation of the fluorescent P-gp substrate Rh-123 was

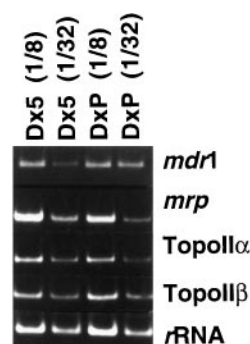


FIG. 2. Analysis of *mdr1*, *mrp*, *Topo II $\alpha$* , and *Topo II $\beta$*  gene expression in DxP cells. Analysis of mRNA expression in DxP and its parental cell line Dx5 using RT-PCR is shown. 28 s rRNA was used as the control gene to normalize expression, and 1/8 or 1/32 in parenthesis denotes serial dilutions of cDNAs. One of at least five independent experiments is presented.

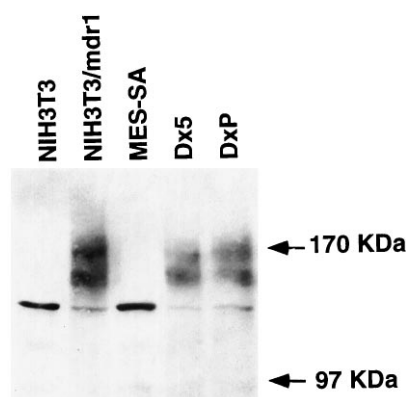


FIG. 3. Western blotting of DxP cells using C219 monoclonal antibody. The whole cell lysates were separated on an 8% SDS-polyacrylamide gel, transferred to membranes, and probed with the C219 antibody (2  $\mu$ g/ml). NIH3T3 and MES-SA cells were used as negative controls, and Dx5 and NIH3T3/*mdr1* (*mdr1* transfected) cells were positive controls for MDR cells.

markedly decreased in Dx5 cells, as expected for MDR cells (Fig. 4). In contrast, DxP cells (although expressing abundant P-gp by UIC2 staining) manifested Rh-123 retention similar to the MDR-negative MES-SA cell line. PSC (2  $\mu$ M) completely restored Rh-123 accumulation in the Dx5 cell line, to levels similar to MES-SA and DxP cells (Fig. 4).

**<sup>3</sup>H-Labeled Drug Accumulation—**Intracellular accumulations of [<sup>3</sup>H]daunorubicin, [<sup>3</sup>H]vinblastine, and [<sup>3</sup>H]cyclosporine were measured to compare the function of P-gp in Dx5 and DxP cells. Both Dx5 and DxP cells displayed similar decreases in [<sup>3</sup>H]daunorubicin accumulation, relative to the MES-SA cell line, while the accumulation of [<sup>3</sup>H]vinblastine was approximately 3-fold higher in DxP than Dx5 cells (Fig. 5, A and B). The decreased drug accumulation in DxP cells was not modulated by PSC, whereas complete modulation was displayed by Dx5 cells (Fig. 5). Uptake of [<sup>3</sup>H]cyclosporine was examined to assess the ability of P-gp to transport the cyclosporins. The intracellular concentration of cyclosporine in DxP cells was equal to that in MES-SA cells and 2-fold higher than in Dx5 cells (Fig. 6). The decreased accumulation of cyclosporine in Dx5 cells was completely modulated by PSC to the levels achieved in DxP and MES-SA cells (data not shown).

**Photoaffinity Labeling with [<sup>125</sup>I]iodoarylazidoprazosin and [<sup>3</sup>H]Azidopine—**DxP cells displayed enhanced photoaffinity binding of P-gp by [<sup>125</sup>I]iodoarylazidoprazosin in the presence of 0.1 and 10  $\mu$ M PSC and vinblastine, in contrast to Dx5 cells in which the photoaffinity labeling was effectively competed by PSC and vinblastine (Fig. 7). The higher concentration (100

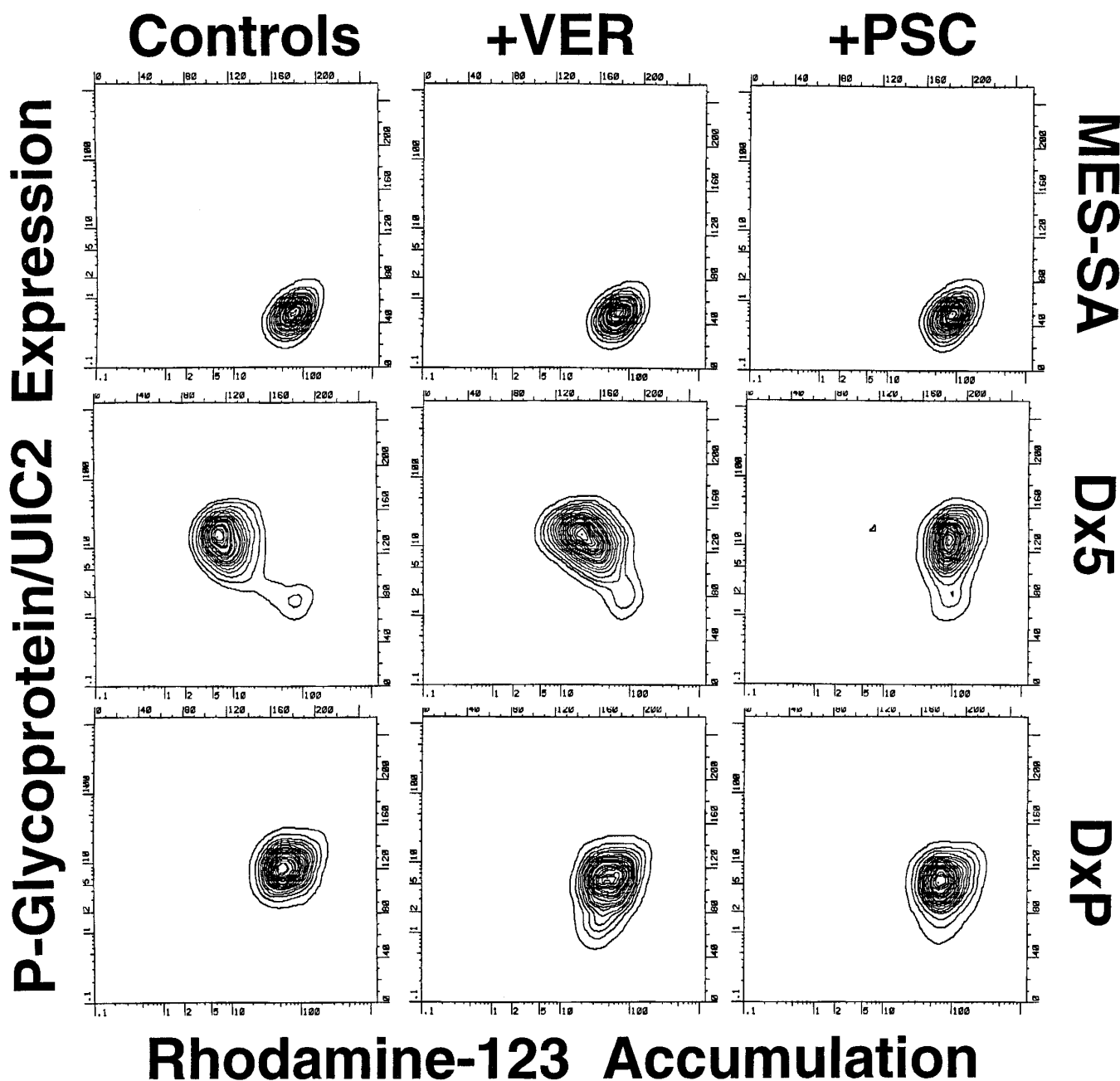


FIG. 4. Functional analysis of Rh-123 retention and P-gp expression in Dxp cells by flow cytometry. Cells were incubated first with rhodamine 123 for 40 min with or without the MDR modulators verapamil (VER) and PSC and then with either the UIC2 antibody or an IgG2a isotype control (40  $\mu\text{g}/\text{ml}$ ) for 20 min and subsequently with Texas Red-conjugated goat anti-mouse IgG2a secondary antibody for another 20 min. The upper panels (MES-SA cells) and middle panels (Dx5 cells) were used as negative and positive controls, respectively, for MDR. The left column depicts cells without MDR modulators, the middle column includes 8  $\mu\text{M}$  verapamil, and the right column includes 2  $\mu\text{M}$  PSC. One of three separate experiments is depicted.

$\mu\text{M}$ ) of PSC or vinblastine abolished detectable P-gp labeling by azidoprazosin in both cell lines. Dxp cells were also resistant to the displacement by PSC or vinblastine of [ $^3\text{H}$ ]azidopine photoaffinity labeling (Fig. 8, A and B). Verapamil was moderately active in both Dxp and Dx5 cells in displacing [ $^3\text{H}$ ]azidopine.

**RT-PCR, DNA Heteroduplex Analysis, and *mdr1* DNA Sequencing**—RT-PCR using primer sets spanning the P-gp coding sequences (Table I) confirmed that the levels of expression of *mdr1* were similar and that the PCR products showed no differences in size when Dx5 and Dxp cells were compared. DNA heteroduplex analysis revealed the formation of a heteroduplex with primers spanning nucleotides 1194–1519 of *mdr1* cDNA, suggesting a sequence difference in transmembrane region 6 (TM6), Fig. 9A. Sequencing of this PCR product identified a

deletion of base pairs 1427–1429 in this region, which encode the amino acid phenylalanine at position 335 of P-gp (Phe<sup>335</sup>) (Fig. 9, B and C). The PCR and sequencing results were reproduced in four different preparations of cDNA from Dxp cells. The deletion of Phe<sup>335</sup> is the only functional mutation in Dxp cells compared with Dx5 and the published human *mdr1* sequence (27). There are other changes from the published *mdr1* sequence that do not alter the P-gp amino acid sequence in Dxp cells: from TCT (Ser) to TCC (Ser) in nucleotide 964 and from ATC (Ile) to ATT (Ile) in nucleotide 3859. These may be polymorphisms of P-gp, since both Dxp and Dx5 have these same substitutions. Amino acid 185 was identified as Gly in both Dx5 and Dxp cells (data not shown).

*Identification of the 1427–1429 TTC Deletion in Genomic*

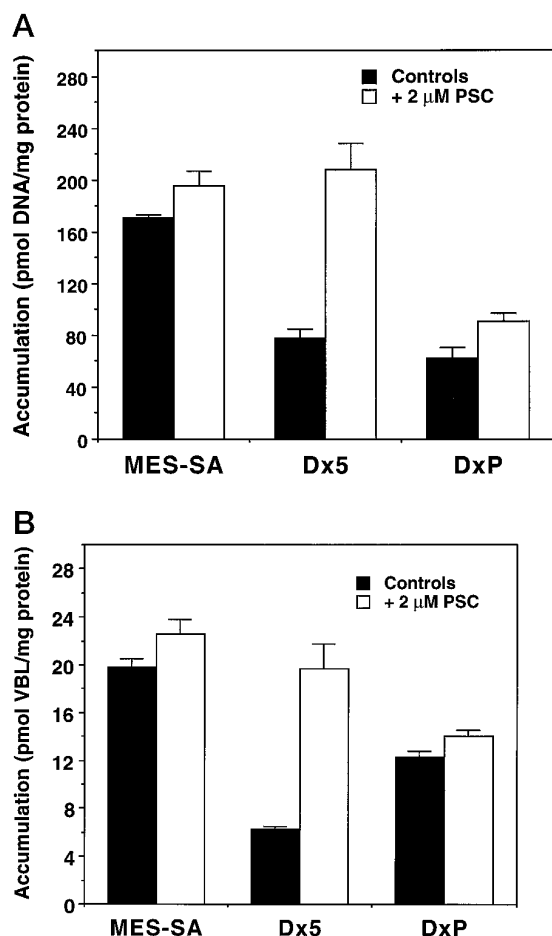


FIG. 5. The effect of PSC on the accumulation of daunorubicin and vinblastine (VBL) in MES-SA, Dx5, and DxP cells. The intracellular accumulations of [<sup>3</sup>H]daunorubicin (A) and [<sup>3</sup>H]vinblastine (B) with or without 2 μM PSC were measured at 37 °C for 60 min. Each point is the mean ± S.D. of triplicate determinations.

**Sequence of DxP Cells**—In order to identify the presence of the mutation in genomic DNA of DxP cells, we amplified genomic DNA using genomic specific primers of *mdr1*. Heteroduplex analysis was performed and revealed that a heteroduplex band existed in DxP but not Dx5 cells. The TTC deletion at codon 335 was also verified by sequencing of the genomic PCR product. Thus, the one-codon deletion was confirmed in DxP cells (Fig. 10).

**Subclonal Analysis of DxP Cells**—Single clones were obtained to analyze the genetic heterogeneity in DxP cells. As shown in Table IV, 11 isolated clones derived from DxP cells showed a similar phenotype including resistance to DOX, resistance to modulation by PSC, and a lower degree of resistance to vinblastine relative to parental Dx5 cells. All tested clones expressed the mutant *mdr1*.

**Mutant *mdr1* Transfection and Cytotoxic Assays**—Plasmids containing wild-type and mutant *mdr1* cDNAs were transfected into drug-sensitive MES-SA cells. Expression of the mutant *mdr1* was confirmed in the appropriate transfectants by DNA heteroduplex analysis. Both wild-type and mutant *mdr1* conferred resistance to doxorubicin, paclitaxel, etoposide, and colchicine. Representative data demonstrating resistance to doxorubicin are shown in Fig. 11A. Exposure of transfectants to both doxorubicin and PSC revealed that only the cells transfected with the mutant *mdr1* bearing the Phe<sup>335</sup> deletion survived, Fig. 11B.

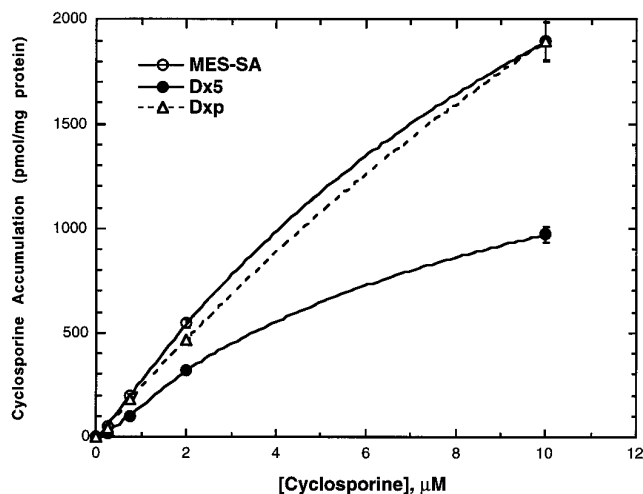


FIG. 6. The accumulation of cyclosporine in MES-SA, Dx5, and DxP cells. The intracellular accumulation of [<sup>3</sup>H]cyclosporine at 0–10 μM extracellular cyclosporine concentrations was measured at 37 °C for 60 min. Each point is the mean ± S.D. of triplicate determinations.

## DISCUSSION

The development of resistance to anticancer drugs is a major impediment to successful chemotherapy, and it is often mediated by the membrane-bound drug-efflux pump, P-gp (1–4). Substances that inhibit P-gp function and reverse the resistance phenotype *in vitro*, termed MDR modulators, have been developed with the intention of administering them in conjunction with MDR-related cytotoxins (9–15). This experiment was designed to examine the resistance mechanisms that arise in MDR cells during multistep selection with DOX, an MDR substrate, and PSC, an effective modulator. A similar selection in non-MDR cells suppressed the activation of *mdr1* and resulted in the emergence of mutants expressing alternative mechanisms of resistance, notably decreased expression of Topo II $\alpha$  (23). Under the conditions of drug exposure in our present experiment, DxP cells displayed cross-resistance to several MDR-related drugs including anthracyclines (DOX and daunorubicin), epipodophyllotoxins (etoposide and teniposide), colchicine, and paclitaxel. However, DxP differed from the parental Dx5 cells in their decreased resistance to *Vinca* alkaloids and lack of cross-resistance to dactinomycin (Table II, Fig. 1). Most notably, the MDR phenotype was not modulated by treatment with the P-gp inhibitor PSC (Table III, Fig. 1).

Although overexpression of *mdr1* is the best characterized mechanism of pleiotropic drug resistance, other mechanisms have been identified. Decreased expression or altered structure of Topo II has been observed in many models of resistance to epipodophyllotoxins, mitoxantrone, and anthracyclines such as DOX (16–18, 23). A membrane ATPase of 190 kDa, distinct from P-gp, has been termed the multidrug resistance-associated protein, encoded by the *mrp* gene, which has been cloned and sequenced in a DOX-selected lung cancer cell line (19). Under our experimental conditions, overexpression of the *mrp* mRNA or significant changes in Topo II $\alpha$  and II $\beta$  were not observed. DxP cells, like the parental Dx5 cells, were not found to express the p110 major vault protein, recognized by the LRP-56 antibody and associated with doxorubicin resistance in some cell models (21). The apparent lack of an alternative resistance mechanism in DxP cells, the residual high expression of P-gp, and the pleiotropic nature of the resistance suggested that a mutant or modified P-gp with decreased affinity for cyclosporins was responsible for the phenotype of these cells.

The altered phenotype of DxP cells correlated very well with

an altered functional activity of P-gp assessed by the cellular uptake of daunorubicin, vinblastine, and cyclosporine. DxP cells displayed a significant decrease in daunorubicin accumulation, which was insensitive to modulation by PSC (Fig. 5A). These cells also exhibited increased vinblastine accumulation compared with Dx5 cells, although the level of this drug was not as high as in drug-sensitive MES-SA cells and was not further increased by PSC (Fig. 5A). The accumulation of cyclosporine in DxP cells was equivalent to that of drug-sensitive MES-SA cells, which do not express P-gp, strongly suggesting an altered affinity of the multidrug transporter for cyclosporins and consistent with the data that cyclosporine and its analogue PSC did not modulate the MDR phenotype of DxP cells (Fig. 6).

As previously reported, compartmentalization or redistribu-

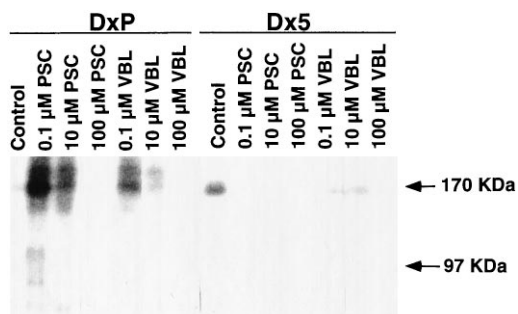


FIG. 7. Photoaffinity labeling of P-gp by [ $^{125}$ I]iodoarylazidoprazosin. [ $^{125}$ I]iodoarylazidoprazosin (10 nM, 81.4 TBq/mmol) was incubated with Dx5 and DxP cell membranes (100  $\mu$ g/reaction) and the indicated concentrations of PSC and vinblastine for 60 min at 25  $^{\circ}$ C. After UV irradiation at 254 nm for 20 min, the samples were solubilized and separated on a 6% SDS-polyacrylamide gel, dried, and autoradiographed. The [ $^{125}$ I]iodoarylazidoprazosin binding was performed with the indicated concentrations of the competitor PSC or vinblastine (VBL).

tion of P-gp leading to redistribution of cytotoxins may result in resistance to modulation (31). Our immunohistochemical experiments localized P-gp to the cell membrane in both Dx5 and DxP. Furthermore, the same amount of P-gp expression and the existence of equivalent daunorubicin accumulation defects in the two cell lines demonstrated that P-gp in DxP cells was capable of transporting some substrates as well as the P-gp in Dx5 cells (Figs. 3, 4, and 5A). The P-gps from the two cell lines have a similar electrophoretic mobility (Fig. 3). Thus, a redistribution or marked structural change in the P-gp expressed in DxP cells was not evident.

Our results identified a novel mutation, consisting of a single codon deletion (Phe $^{335}$ ) in the TM6 region of P-gp in DxP cells. The drug resistance phenotype we observed is similar, in some respects, to that described in a previously published report of the functional consequences of a substitution for the phenylalanine at codon 335 by site-directed mutagenesis, which resulted in decreased dactinomycin resistance (32). The expression of this mutant P-gp in DxP cells is probably the result of selection of a spontaneously arising mutant or selective allelic expression of an *mdr1* gene that confers a PSC-resistant MDR phenotype. Karyotyping and fluorescent *in situ* hybridization analysis of chromosome 7 revealed no obvious alterations in chromosome structure in DxP cells.

The deletion of codon 335 as a mechanism of resistance to modulation of MDR by cyclosporins may be an extremely rare event. We have not found a similar mutation in 13 other mutants separately derived from MES-SA cells that were co-selected by DOX and PSC, with a mutation rate of  $2.5 \times 10^{-7}$  per cell generation (23). Those mutants were resistant to DOX and PSC on the basis of a down-regulation of Topo II $\alpha$  expression. The MES-SA cells used in that experiment do not express *mdr1*, whereas the MDR variant Dx5 cells used to select the

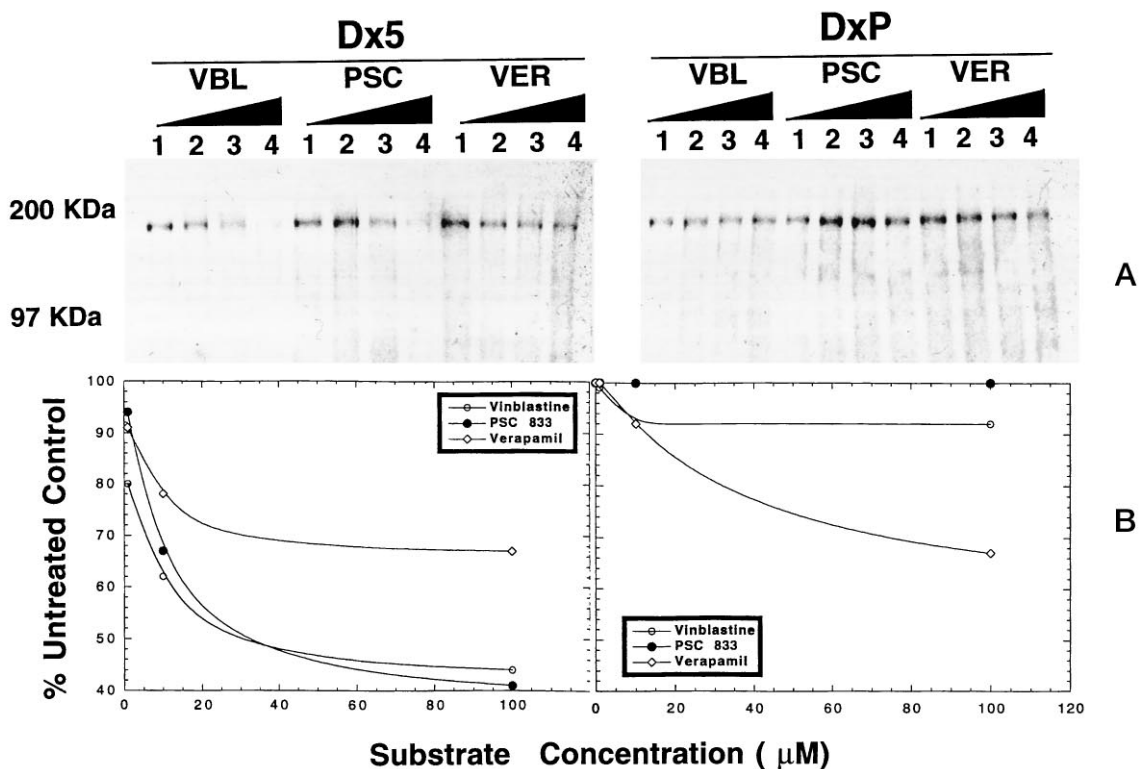
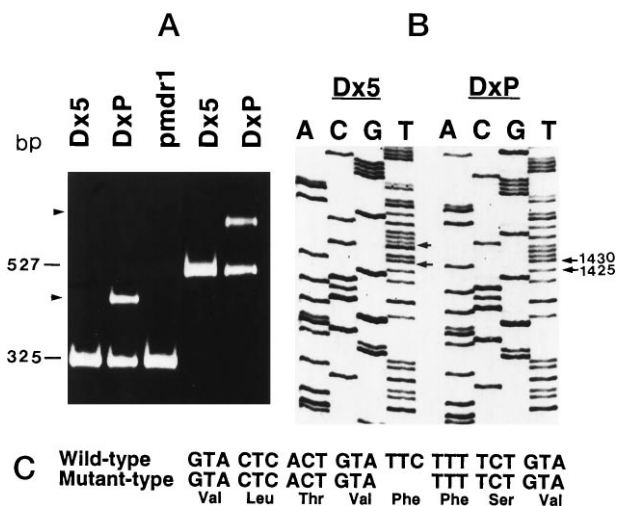
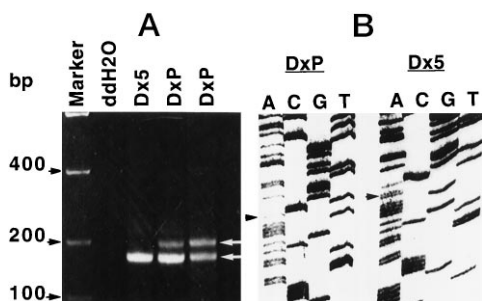


FIG. 8. Photoaffinity labeling of P-gp (P170) by [ $^3$ H]Azidopine. [ $^3$ H]Azidopine (50 nM) was incubated with Dx5 and DxP membranes (100  $\mu$ g/reaction) and the indicated concentrations of the competitors PSC, verapamil (VER), or vinblastine (VBL) for 60 min at 25  $^{\circ}$ C. After UV irradiation at 254 nm, the samples were solubilized and separated on a 6% SDS-polyacrylamide gel, dried, and autoradiographed. A, fluorography, with 1, 2, 3, and 4 representing concentrations of the competitors of 0, 1, 10, and 100  $\mu$ M. B, quantitation of the results of A by digitized image analysis.



**FIG. 9. Demonstration of the amino acid 335 codon deletion in P-gp by heteroduplex analysis and sequencing of RT-PCR products of *mdr1* cDNA from Dx5 and DxP cells.** A, DNA heteroduplex analysis. The 325-base pair (lanes 1–3) and 527-base pair (lanes 4 and 5) RT-PCR products were obtained by using two different primer sets spanning the TM6 region of *mdr1*. Pmdr1 is a plasmid containing the wild-type *mdr1* gene. The 5- $\mu$ l post-PCR reactions were mixed with 5  $\mu$ l of Dx5 (wild type) RT-PCR products, denatured at 95 °C, and allowed to reanneal by reducing the temperature to 25 °C over 30 min. An MDE<sup>TM</sup> gel was stained with ethidium bromide, and the desired products were located on an ultraviolet transilluminator, photographed, and quantified. Arrows indicate the heteroduplex bands. B, sequencing analysis of the RT-PCR products. The arrows indicate the mutation site. The TTC (1427–1429) was deleted in all analyzed DxP cDNA samples. One of five independent experiments is shown. C, the cDNA sequences of *mdr1* from the Dx5 (wild type) and DxP cells (with deletion of the amino acid 335 phenylalanine codon).



**FIG. 10. Demonstration of the amino acid 335 codon deletion in genomic DNA of DxP cells.** PCR was performed on genomic DNA treated with RNase, and the PCR products of Dx5 and DxP were annealed with Dx5 as described in the legend to Fig. 9. A 12% polyacrylamide gel was stained with ethidium bromide, and desired products were located on an ultraviolet transilluminator, photographed, and quantified. A, the upper arrow indicates the heteroduplex bands. The heteroduplex bands in lane 4 were reamplified, and DNA heteroduplex analysis was repeated (lane 5, DxP). B, the homoduplex band (Fig. 10A, lower band of lane 5) was purified from an 8% polyacrylamide gel and subcloned into the pGEM-T vector (Promega). Individual clones were selected for sequencing. The arrows indicate the mutation site. The TTC codon for amino acid 335 was deleted in all analyzed DxP genomic inserts.

DxP variant with DOX and PSC actively transcribed *mdr1*, a factor that may have contributed to the selection of a mutant P-gp rather than to an alternative mechanism of resistance such as altered Topo II expression.

Several point mutations or polymorphisms of *mdr1* have been identified in different species including hamsters, mice, and humans (reviewed in Ref. 33; Refs. 34–38). Some of these have been associated with an altered phenotype, such as the substitution from Gly<sup>185</sup> to Val<sup>185</sup> in human P-gp, which confers preferential resistance to colchicine (36, 37). The colchicine

**TABLE IV**  
Drug resistance phenotypes of subclones of DxP cells

Cells	DOX <sup>a</sup>	DOX + PSC	VBL <sup>b</sup>	VBL + PSC	<i>mdr1</i> <sup>c</sup>
Controls					
MES-SA	1	1	1	0.5	Negative
Dx5	80	1	243	1	WT
DxP	77	53	14	12	Mut
Subclones <sup>d</sup>					
Dx/PAS	163	51	15	5	Mut
Dx/PBS	67	13	3	1	ND <sup>e</sup>
Dx/PCS	50	23	8	3	Mut
Dx/PDS	150	100	20	6	Mut
Dx/PES	96	100	3	1	Mut
Dx/PFS	150	75	21	8	ND
Dx/PGS	7	7	2	1	ND
Dx/PHS	83	37	ND	ND	ND
Dx/PIS	13	3	2	1	Mut
Dx/PJS	175	75	19	10	ND
Dx/PMS	100	50	5	2	Mut

<sup>a</sup> The numbers represent -fold resistance relative to control, drug-sensitive MES-SA cells as determined by the MTT assay.

<sup>b</sup> VBL, vinblastine.

<sup>c</sup> Identification of *mdr1* gene expression by RT-PCR and DNA heteroduplex assay. WT, wild-type *mdr1*; Mut, mutant *mdr1* mRNA (deletion of the codon for amino acid 335).

<sup>d</sup> Subclones of DxP were obtained by limiting dilution of cell populations in 96-well plates. The clones were maintained in drug-free conditions over 2 months and were tested for their drug resistance phenotypes.

<sup>e</sup> ND, not determined.

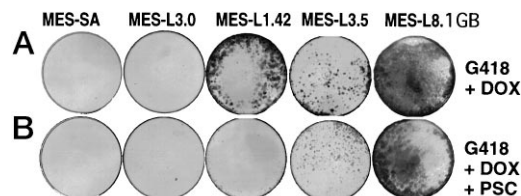


**FIG. 11. Cytotoxic effect on *mdr1* transfectants.** The MES-SA cells were transfected with plasmid vectors pcDNA3 (vector control) and pcDNA3 containing *mdr1* inserts by electroporation (30). MES-L3.0, MES-L1.42, MES-L3.5, and MES-L8.1 represent MES-SA cells transfected with pcDNA3 vector, wild-type *mdr1* plasmid (pcDMDR1.4), pcDMDR3.5 (deletion of Phe<sup>335</sup> of pcDMDR1.4), and pcDMDR8.1 (mutant *mdr1* with Phe<sup>335</sup> deletion isolated from the DxP cDNA library), respectively. The freshly isolated G418-resistant bulk cells ( $2 \times 10^4$ /well) were incubated with medium containing G418 (400  $\mu$ g/ml) and DOX (22 nM) for 1 week (A), and the parallel wells were further treated with 2  $\mu$ M PSC for another week (B). The cells surviving drug treatment were stained by MTT and are shown in this figure as dark colonies. Only those viable cells with intact mitochondria were capable of metabolizing the MTT into the formazan crystals. The dishes were then photographed.

selection of KB cells in this case may have favored overexpression of one allele of *mdr1* and suggests that codon 185 in human P-gp may be subjected to DNA polymorphism. Both Dx5 and DxP cells express the Gly<sup>185</sup>. The impact of structural alterations of P-gp on modulation of MDR by inhibitors is poorly understood (9, 32, 33, 38).

The novel mutation we have identified in this study (deletion of Phe<sup>335</sup>) provides insight into the relationship between P-gp structure and modulation of MDR by cyclosporins. Our data support the theory that a specific ligand-receptor mechanism is involved in P-gp-mediated MDR. PSC and cyclosporine are known to bind to P-gp, and cyclosporine is a transport substrate for P-gp. Phenylalanine and other aromatic residues are preferentially located at the cytoplasmic boundaries, where they are thought to position the transmembrane segments. Several such residues, including Phe<sup>335</sup>, Phe<sup>777</sup>, and Phe<sup>978</sup>, are thought to be of functional importance in P-gp (32). Substitution of a nonaromatic residue for Phe<sup>335</sup> substantially impairs the ability of the transporter to confer resistance to

vinblastine and dactinomycin, while the ability to confer resistance to DOX and colchicine is preserved (32).

DxP cells showed enhanced iodoarylazidoprazosin labeling in the presence of both PSC and vinblastine and decreased ability of either PSC or vinblastine to replace the P-gp probe (Fig. 7). Photoaffinity experiments have localized azidopine binding domains in P-gp to TM5-6 or to TM6 and TM12 (reviewed in Ref. 33). Previous experiments have demonstrated that the two halves of P-gp come together to form a single site for drug binding, involving the TM5-6 and TM11-12 regions (33). Additional data suggest that azidopine and vinblastine may not bind to the same site (33, 39) and that conformational or allosteric effects could be responsible for the inhibition of labeling by azidopine in the presence of vinblastine. The collateral increased affinity to iodoarylazidoprazosin labeling in DxP cells may be due to an allosteric effect of the deletion of Phe<sup>335</sup>. The deletion of Phe<sup>335</sup> in the P-gp expressed by DxP cells resulted in loss of the capacity to bind or transport cyclosporine, PSC, and vinblastine. Our results suggest that cyclosporine, PSC, vinblastine, Rh-123, and dactinomycin share at least one binding domain on P-gp (Tables II and III, Figs. 4-7). These results indicate that this residue plays an important role in the interaction of P-gp with cyclosporine and PSC.

Our results do not completely rule out the existence of other modifying factors that may directly or indirectly affect the multidrug resistance phenotype in DxP cells, although no obvious alternative mechanism was observed. Several major known alternative mechanisms of resistance to DOX were not different between Dx5 and DxP cells. Moreover, the clonal analysis of the DxP cell population supported the association of the mutant P-gp expression with resistance to modulation by PSC and decreased cross-resistance to vinblastine in every subclone tested (Table IV). Finally, transfection of the mutant *mdr1* gene conferred a drug resistance phenotype that was resistant to modulation by PSC (Fig. 11).

In summary, our data reveal a functionally important mutation of P-gp arising from co-selection of *mdr1*-positive cells with DOX and PSC. The resistance phenotype of the resulting DxP cell line may be attributed to the deletion of Phe<sup>335</sup> from P-gp. Our data suggest that the phenylalanine residue at codon 335 may be important in the binding and transport of cyclosporins by P-gp and to their ability to modulate MDR. In addition, this mutation results in decreased resistance to *Vinca* alkaloids, lack of cross-resistance to dactinomycin, and markedly decreased ability to transport Rh-123.

**Acknowledgments**—We are grateful to Dr. Igor Roninson for valuable suggestions and comments. We thank Eva Pfendt, Mary Kovacs, Dana Bangs, and Dr. Yan Wang for excellent technical assistance.

#### REFERENCES

- Ling, V. (1992) *Cancer* **69**, 2603-2609
- Roninson, I. B. (1991) *Molecular and Cellular Biology of Multidrug Resistance in Tumor Cells*, Plenum Press, New York, NY
- Gottesman, M. M. (1993) *Cancer Res.* **53**, 747-754
- Fisher, G. A., and Sikic, B. I. (1995) in *Hematol. Oncol. Clin. North Am.* **9**, 363-382
- Goldstein, L. J., Galski, H., Fojo, A., Willingham, M., Lai, S.-L., Gazdar, A., Pirker, R., Green, A., Crist, W., Brodeur, G. M., Lieber, M., Cossman, J., Gottesman, M. M., and Pastan, I. (1989) *J. Natl. Cancer Inst.* **81**, 116-124
- Chan, H. S. L., Thorner, P. S., Haddad, G., and Ling, V. (1990) *J. Clin. Oncol.* **8**, 689-704
- Marie, J.-P., Zittoun, R., and Sikic, B. I. (1991) *Blood* **3**, 586-592
- Holzmayr, T. A., Hilsenbeck, S., Von Hoff, D. D., and Roninson, I. B. (1992) *J. Natl. Cancer Inst.* **84**, 1486-1491
- Sikic, B. I. (1993) *J. Clin. Oncol.* **11**, 1629-1635
- Dalton, W. S., Grogan, T. M., Meltzer, P. S., Scheper, R. J., Durie, B. G. M., Taylor, C. W., Miller, T. P., and Salmon, S. E. (1989) *J. Clin. Oncol.* **7**, 415-424
- Sonneveld, P., and Nooter, K. (1990) *Br. J. Haem.* **75**, 208-211
- Arceci, R. (1993) *Blood* **81**, 2215-2222
- Boesch, D., Gavériaux, C., Jachez, B., Pourtier-Manzanedo, A., Bollinger, P., and Loor, F. (1991) *Cancer Res.* **51**, 4226-4233
- Boesch, D., Muller, K., Pourtier-Manzanedo, A., and Loor, F. (1991) *Exp. Cell Res.* **196**, 26-32
- Yahanda, A. M., Adler, K. M., Fisher, G. A., Brophy, N. A., Halsey, J., Hardy, R. L., Gosland, M. P., Lum, B. L., and Sikic, B. I. (1992) *J. Clin. Oncol.* **10**, 1624-1634
- Liu, L. F. (1989) *Annu. Rev. Biochem.* **58**, 351-375
- Beck, W. T. (1990) *Cancer Treat. Rev.* **17**, 11-20
- Kasahara, K., Fujiwara, Y., Sugimoto, Y., Nishio, K., Tamura, T., Matsuda, T., and Saijo, N. (1992) *J. Natl. Cancer Inst.* **84**, 113-118
- Cole, S. P. C., Bhardwaj, G., Gerlach, J. H., Mackie, J. E., Grant, C. E., Almquist, K. C., Stewart, A. J., Kurz, E. U., Duncan, A. M. V., and Deeley, R. G. (1992) *Science* **258**, 1650-1654
- Zaman, G. J. R., Versantvoort, C. H. M., Smit, J. J. M., Eijdeems, E. W. H. M., de Haas, M., Smith, A. J., Broxterman, H. J., Mulder, N. H., de Vries, E. G. E., Baas, F., and Borst, P. (1993) *Cancer Res.* **53**, 1747-1750
- Scheper, R. J., Broxterman, H. J., Scheffer, G. L., Kaaijk, P., Dalton, W. S., van Heijningen, T. H. M., van Kalken, C. K., Slovak, M. L., de Vries, E. G. E., van der Valk, P., Meijer, C. J. L. M., and Pinedo, H. M. (1993) *Cancer Res.* **53**, 1475-1479
- Chen, G., Jaffrézou, J.-P., Fleming, W. H., Durán, G. E., and Sikic, B. I. (1994) *Cancer Res.* **54**, 4980-4987
- Bekecic-Oreskovic, L., Durán, G. E., Chen, G., Dumontet, C., and Sikic, B. I. (1995) *J. Natl. Cancer Inst.* **87**, 1593-1602
- Harker, W. G., MacKintosh, F. R., and Sikic, B. I. (1983) *Cancer Res.* **43**, 4943-4950
- Harker, W. G., and Sikic, B. I. (1985) *Cancer Res.* **45**, 4091-4096
- Sasai, K., Evans, J. W., Kovacs, M. S., and Brown, J. M. (1994) *Int. J. Radiat. Oncol. Biol. Phys.* **30**, 1127-1132
- Chen, C., Clark, D., Ueda, K., Pastan, I., Gottesman, M. M., and Roninson, I. B. (1990) *J. Biol. Chem.* **265**, 506-514
- Chambers, T. C., McAvoy, E. M., Jacobs, J. W., and Eilon, G. (1990) *J. Biol. Chem.* **265**, 7679-7686
- Jaffrézou, J.-P., Chen, G., Durán, G. E., Muller, C., Bordier, C., Laurent, G., Sikic, B. I., and Levade, T. (1995) *Biochim. Biophys. Acta.* **1266**, 1-8
- Baum, C., Foster, P., Hegewisch-Becker, S., and Harbers, K. (1994) *Biotechniques* **17**, 1058-1062
- Abbaszadegan, M. R., Cress, A. E., Futscher, B. W., and Dalton, W. S. (1995) *Proc. Am. Assoc. Cancer Res.* **36**, 330
- Loo, T. W., and Clarke, D. M. (1993) *J. Biol. Chem.* **268**, 19965-19972
- Greenberger, L. M., Cohen, D., and Horwitz, S. B. (1994) *Cancer Treat. Res.* **73**, 69-106
- Gros, P., Dhir, R., Croop, J., and Talbot, F. (1991) *Proc. Natl. Acad. Sci. U. S. A.* **88**, 7289-7293
- Devine, S. E., Ling, V., and Melera, P. W. (1992) *Proc. Natl. Acad. Sci. U. S. A.* **89**, 4564-4568
- Choi, K., Chen, C., Krieglner, M., and Roninson, I. B. (1988) *Cell* **53**, 519-529
- Safa, A. R., Stern, R. K., Choi, K., Agresti, M., Tamai, I., Mehta, N. D., and Roninson, I. B. (1990) *Proc. Natl. Acad. Sci. U. S. A.* **87**, 7225-7229
- Kajiji, S., Dreslin, J. A., Grizzuti, K., and Gros, P. (1994) *Biochemistry* **33**, 5041-5048
- Tamai, I., and Safa, A. R. (1991) *J. Biol. Chem.* **266**, 16796-16800